Appl. Phys. B 81, 1091–1096 (2005)
DOI: 10.1007/s00340-005-2028-6

Applied Physics B
Lasers and Optics

A. BAUM[1]
D. GREBNER[1]
W. PAA[1,✉]
W. TRIEBEL[1]
M. LARIONOV[2]
A. GIESEN[2]

Axial mode tuning of a single frequency Yb:YAG thin disk laser

[1] Institut für Physikalische Hochtechnology (IPHT), Albert-Einstein-Strasse 9, 07745 Jena, Germany
[2] Institut für Strahlwerkzeuge (IFSW), Pfaffenwaldring 43, 70569 Stuttgart, Germany

Received: 23 April 2005/Revised version: 31 August 2005
Published online: 5 November 2005 •

ABSTRACT We describe an arrangement for an Yb:YAG thin disk laser, which enables narrow bandwidth operation in single-frequency mode at freely selectable wavelengths within the broad tuning range of the laser. This is facilitated by a combination of a double-stage birefringent filter and an etalon inside the laser cavity. We investigate the wavelength selection characteristics of the single elements as well as their combination. A simple procedure is implemented for a computer-based automation of wavelength tuning. The reflectivity of the partially reflecting resonator mirror is optimised, and the laser pump power is adapted for best tuning performance. Single-frequency emission is achieved in a frequency range of 9.75 THz (wavelength range 1020 nm to 1055 nm). Each axial laser mode in this range can be selected individually. The axial mode separation of 0.47 GHz corresponds to wavelength steps of 1.7 pm at 1030 nm.

PACS 42.55.Xi; 42.60.Fc; 42.60.Lh

1 Introduction

The range of applications of laser based diagnostics is steadily growing and covers a huge field of scientific and industrial interests, e.g., measurement of material properties, process diagnostics or combustion research. Among the vast variety of special methods such as particle image velocimetry (PIV), Raman-scattering, MIE-scattering and laser induced incandescence (LII), laser induced fluorescence (LIF) plays an important role [1]. For this method narrow-band, continuously tunable light sources with a broad tuning range are essential. The process diagnostics require compact and efficient laser sources, especially in experimental conditions such as microgravity [2]. Moreover, a high repetition rate is highly desirable, since it enables tracking processes of turbulence or ignition over a much shorter time scale than with conventional lasers, such as excimer or dye lasers. The ideal laser sources concerning efficiency, ease of use and compactness are pulsed diode pumped solid state lasers (DPSSL). However, to date commercial DPSSLs cannot simultaneously deliver high repetition rates (kHz range), tunable, narrow-band operation and high pulse energies (several tens of mJ). Thus, a novel DPSSL for laser diagnostics was developed based on a thin disk laser. This promising novel laser architecture delivers high output power combined with high beam quality as well as high pulse energies [3, 4]. In combination with Yb:YAG as active laser material, excellent beam profile, efficiency and tunability could be demonstrated [5, 6]. All the above requirements can be facilitated with a two stage Yb:YAG master oscillator power amplifier laser system. The first stage supplies narrow-band tunable laser emission, used as seed radiation in a pulsed operating regenerative amplifier system. The output pulses of that second stage are frequency converted to the UV spectral range for selective excitation of combustion products [7, 8]. To obtain spectrally well defined seed radiation in the first stage, laser operation of only one axial mode is required (single frequency regime). Moreover, each single axial laser mode inside the broad tuning range (from 1020 nm to 1055 nm) should be selectable for continuous tunability. Narrow band excimer lasers, for example, usually employ a diffraction grating, often in combination with etalons, to reach this aim. In our case, however, the comparable low gain coefficient of Yb:YAG prohibits this approach. The large losses of the grating would prevent the laser from emitting. Consequently, we investigated alternatives that minimise losses. The most preferable approach, in our opinion, is the intracavity combination of birefringent filters and an etalon as wavelength selective elements. This solution, which is also ideal for automation, is studied in detail in this paper.

2 Setup and operation

The Yb:YAG thin disk laser head features the pump optic, focusing the pump radiation of a laser diode stack (InGaAs at 940 nm) onto a 200 μm thick Yb:YAG disk. The rear side of the disk, which is mounted on a heat sink, is coated for high reflectivity. Together with a partially reflecting, curved output coupler (3 m radius), it constitutes the laser cavity [9]. The spatial mode structure of the disk laser is nearly diffraction limited. This is also valid for high pump power values due to the well defined pump spot on the surface of the disk and the efficient, quasi one-dimensional cooling mechanism. The length of the resonator determines the formation of axial modes and their separation (0.47 GHz for 320 mm resonator length). Since in this configuration different modes

✉ Fax: +49 3641 206-499, E-mail: wolfgang.paa@ipht-jena.de

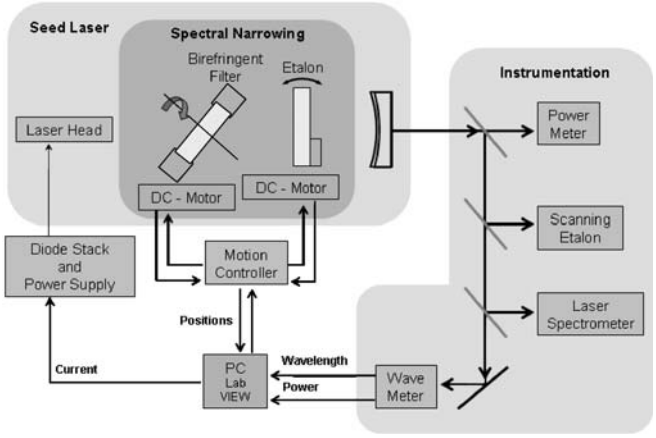

FIGURE 1 Schematic of the seed laser including wavelength selective elements for spectral narrowing and setup of instrumentation, power supply and motion control for automated wavelength tuning

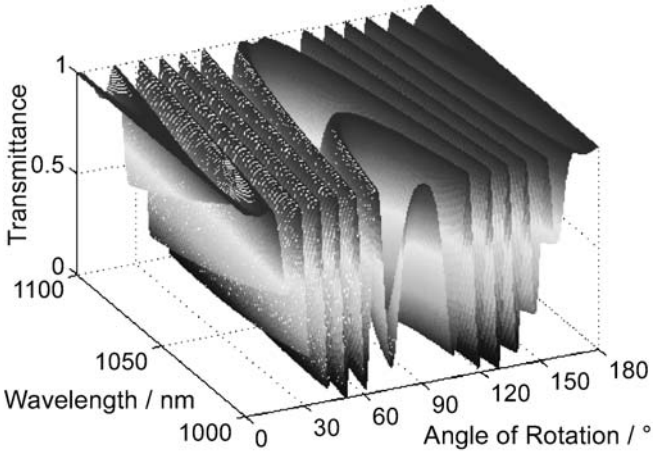

FIGURE 2 Transmittance of a 2 mm thick quartz birefringent filter in dependence of wavelength and angle of rotation (crystal cut with its optical axis parallel to surface)

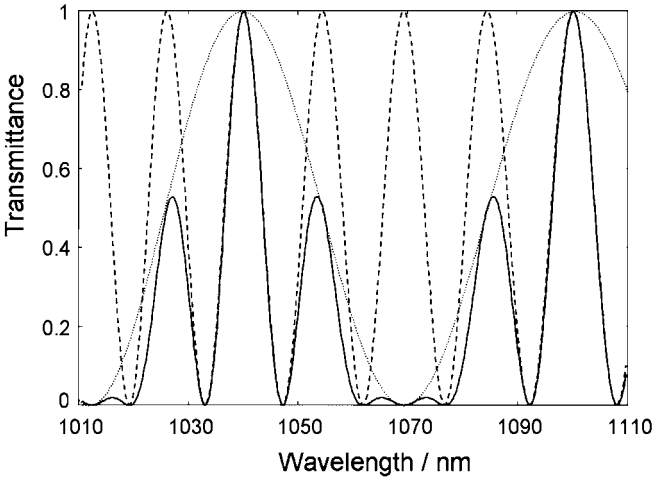

FIGURE 3 Transmittance curves of two birefringent filters (*dashed line*: 8 mm thickness, *doted line*: 2 mm thickness, *solid line*: transmittance product)

compete, frequency selective elements have to be inserted into the resonator to suppress unwanted modes. Figure 1 shows a schematic of the experimental arrangement. It anticipates the finalised setup for tuning the wavelength via a computer and characterising the output parameters of the laser. The power meter and the wavelength measuring devices (wave meter, scanning etalon and laser spectrometer) provide feedback to control the orientation of the spectrally selective elements (birefringent filter, etalon) as well as the pump power via a LabVIEW program. The wavelength is measured by a spectrometer (frequency range 11 THz) to survey the whole tuning range of 9.75 THz at once, a scanning etalon (free spectral range 7.5 GHz), which provides sufficient resolution to separate axial laser modes, and a wave meter (Michelson interferometer, spectral resolution 0.28 GHz), which enables data transfer to the computer. Since the tuning algorithm receives input only from the wave meter, the other devices can be omitted for a properly adjusted laser.

We investigate a combination of birefringent filters and an etalon as wavelength selectors. In the birefringent filter (crystalline quartz) incident light is split in two perpendicular directions of polarisation. The ordinary and extraordinary rays propagate with different velocities through the material. The refractive index in the extraordinary direction varies depending on the angle of incidence relative to the optical axis of the crystal. Therefore, a variable phase difference between both rays is introduced, which depends on the orientation of the birefringent filter (rotation relative to the optical axis) and the wavelength [10, 11]. In order to dictate a dominant direction of polarisation, and therefore select or suppress different axial modes according to the introduced phase difference, the birefringent filter is placed at Brewster's angle within the cavity. The reflection of light, polarised parallel to the plane of incidence, is zero. Thus, light with this direction of polarisation suffers substantially lower losses. Therefore, the resonator internal transmittance of parallel polarised light through the element is a function of the filter's angle of rotation. The transmittance is maximal for the particular wavelength when only parallel polarised light passes the crystal. To illustrate this behaviour, the calculated transmittance of parallel polarised light through a 2 mm thick birefringent filter is shown in Fig. 2. The regions of maximum transmittance form several hyperbolic structures. These relate the wavelengths, which suffer the lowest losses, to the appropriate angle of rotation of the element. The highest wavelength selectivity can be found in the regions between the non wavelength-selective positions at 0°, 180° and the turning points of the hyperbola, where the incident light propagates as either an ordinary or an extraordinary ray. In the case that the crystal is cut with its optical axis oriented parallel to its surface, these points occur at 90°. The optimum angle of rotation is, in this case, near 45°. The linear tuning dependence in this region simplifies the automated tuning procedure. In Fig. 3 transmittance curves of two birefringent filters at fixed orientation (angle of rotation) are shown. Their thickness is 8 mm and 2 mm, respectively. We note that the thickness directly relates to the number as well as to the full width at half maximum (FWHM) of the transmittance bands. The birefringent filter of 2 mm thickness suppresses wavelengths that are more distant from the selected wavelength but still within the gain region of Yb:YAG (1020–1060 nm). When the desired wavelength is near the minimum gain of Yb:YAG at 1040 nm, it

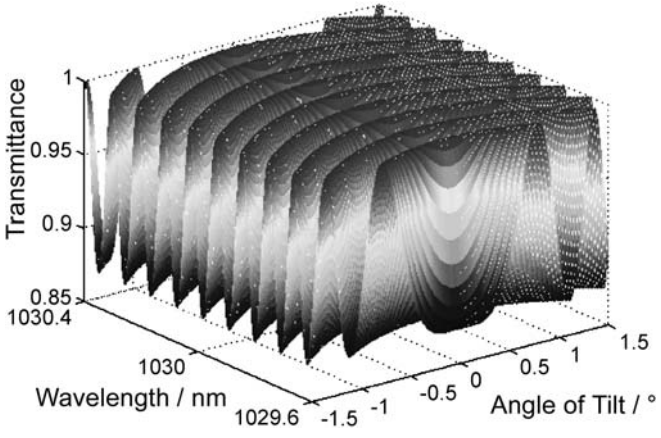

FIGURE 4 Transmittance of a 4 mm thick etalon in dependence of wavelength and angle of tilt

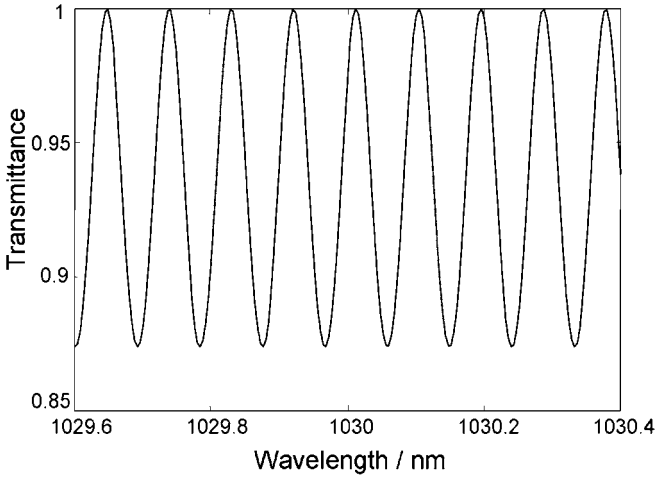

FIGURE 5 Transmittance curve of an etalon (4 mm thickness)

inserts losses of about 30% for wavelength at ±10 nm distance. This is sufficient to suppress laser operation at the maximum gain around 1030 nm. However, wavelengths very close to the maximum transmittance cannot be suppressed efficiently. In contrast, a birefringent filter of 8 mm thickness provides a four times smaller FWHM, causing much higher losses for adjacent wavelengths. However, it also allows operation of wavelengths other than the selected one. For this reason, it is necessary to combine these two elements, resulting in a new transmittance curve, which is the product of the transmittance curves of both components (solid line in Fig. 3). This yields a reduced spectral width of the transmittance maximum, neighboured by different, strongly suppressed, distant wavelengths. For automated wavelength selection it is advantageous to mount both filters with a small air gap together in a fixed position. This reduces the number of moveable components. Therefore, it is essential that the thickness ratio of the different elements takes an integer value to match the transmittance maxima and to minimise the intracavity losses [13].

In addition to the birefringent filter, a second element is required to ensure single axial mode operation. Since the transmission bands of the birefringent filter are broad, the laser may switch between several axial modes. Therefore, an uncoated etalon was chosen to suppress other axial modes than the desired. The etalon uses multiple reflection interference inside a fused silica plate for wavelength selection [12]. The refractive index of the material, the angle of incidence and the actual thickness of the element determine several resonant frequencies. These regions of maximum transmittance are symmetrically grouped, with respect to 0° angle of tilt and are separated by the free spectral range (FSR) of the element as illustrated in Fig. 4. The introduced change in resonator length by tilting the etalon is negligible (e.g., 4 mm thick etalon tilted by 2° causes 0.18 μm change in resonator length, corresponding to a shift of 216 Hz (4.6×10^{-5}%) in axial mode spacing). However, a spatial displacement of the beam occurs (47 μm for 2° tilted, 4 mm thick etalon) causing additional losses if not compensated. The transmission curve of a 4 mm thick etalon for perpendicular incidence is shown in Fig. 5. Although the etalon of 4 mm thickness introduces only very small losses for adjacent axial modes (3.57×10^{-2}% loss at a corresponding frequency difference of 0.47 GHz), a suppression of these frequencies is demonstrated experimentally when used together with the birefringent filters. This takes advantage of the effect of spatial hole burning in the active medium of the thin disc laser, which is explained in the following section.

3 Results and discussion

Figure 6 shows the spectrum of the Yb:YAG laser, operated far above laser threshold and without any wavelength restriction. Four different wavelengths are amplified (1029.5 nm, 1030.5 nm, 1031.25 nm and 1031.75 nm), which are located within the region of maximal gain of the active medium. Obviously, these are not adjacent axial modes. Inside an ideally homogeneously broadened laser medium only one wavelength, which experiences the highest gain, may oscillate. However, due to the effect of spatial hole-burning several axial modes may coexist, which are able to benefit from different spatial regions of inversion. When the laser medium is placed in the middle of the resonator, adjacent axial modes are able to utilise the inversion since they form mutually inverse spatial structures. In contrast, in the thin disk laser the active medium is located at one totally reflecting mirror.

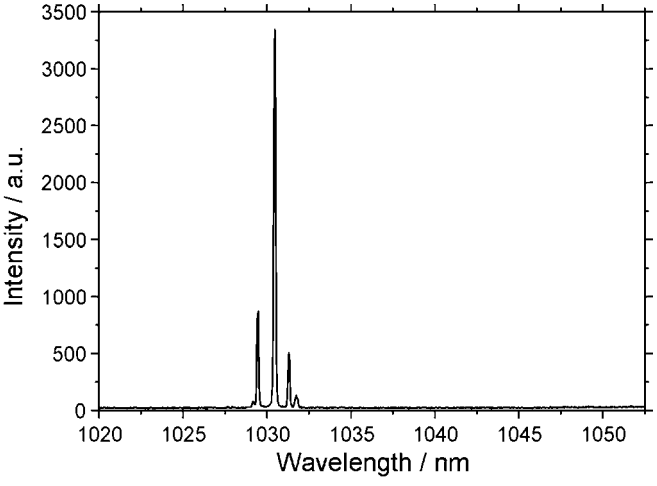

FIGURE 6 Intensity distribution of the laser emission of the Yb:YAG disk laser without any wavelength selective elements inside the cavity

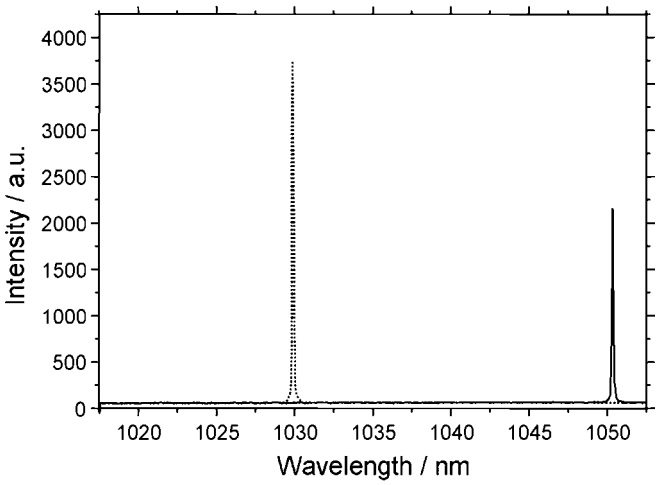

FIGURE 7 Intensity distribution of the laser emission after integration of the two stage birefringent filter at two different angles of rotation

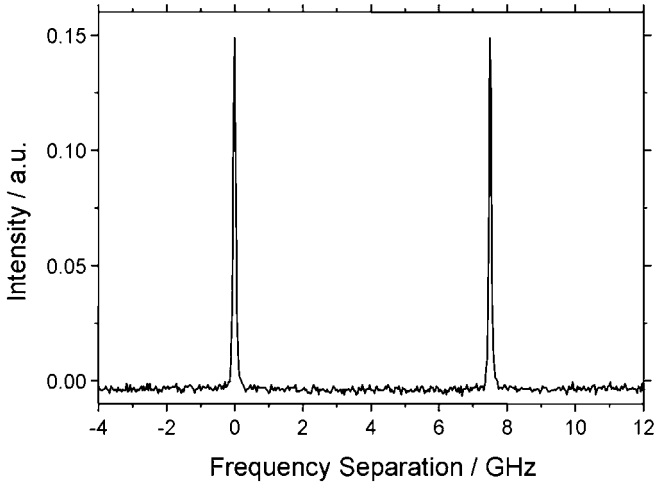

FIGURE 8 Intensity distribution of the laser emission with application of the two-stage birefringent filter and the 4 mm thick etalon; restriction to a single axial mode

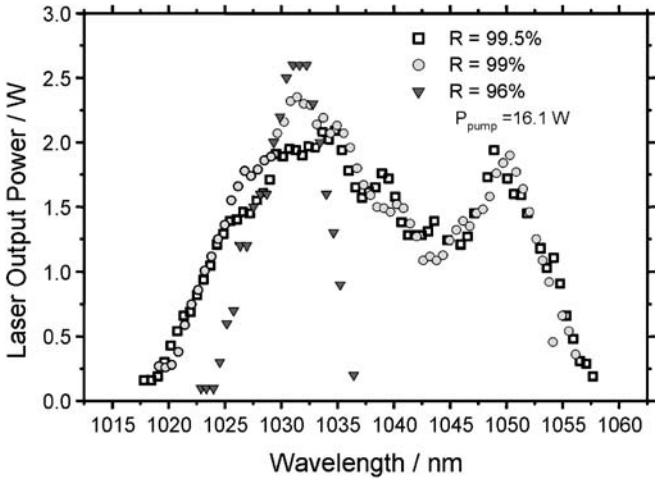

FIGURE 9 Tuning curves for different values of the reflectivity R of the output coupler

Here, the electromagnetic fields of adjacent axial modes are almost similar and prevent their coexistence [14]. Thus, separated wavelengths oscillate and benefit from high gain such as present in Fig. 6.

The effect of the insertion of the two stage birefringent filter into the resonator is shown in Fig. 7 with two spectra for different angles of rotation of the element. The two stage birefringent filter suppresses unwanted wavelengths and limits the emission bandwidth to below 7 THz (25 pm at 1030 nm; resolution of laser spectrometer). Nevertheless, it is not sufficient for stable single axial mode operation and hopping between adjacent modes could be observed with a scanning etalon. Fixation of the laser emission to one axial mode could be accomplished by the addition of a 4 mm thick etalon. Although the introduced losses for adjacent modes are very small, the same effect of spatial hole burning as seen in the spectrum without wavelength selective elements (Fig. 6) helps to prevent laser oscillation at other modes than the selected. In contrast to the performance of the two-stage birefringent filter alone, where several modes in the selected region were permanently competing, stable single frequency operation was obtained using the etalon. Figure 8 depicts the restriction of the laser emission to one exclusive axial mode, measured with a scanning etalon. The device displays repeatedly multiples of its measured free spectral range of 7.5 GHz. The measurement of the laser threshold, which increased only marginally (0.1 W at 1030 nm), showed that only very low overall losses were added by the material of the selective elements. However, the slope efficiency decreased (from 26.3% to 18.4% at 1030 nm) due to restricted spectral components of the laser emission, and therefore the output power of the system declined. Since the gain of the active medium varies with wavelength, the reflectivity of the output coupler was optimised for wavelengths with low gain around 1040 nm. In Fig. 9 tuning curves using different values of reflectivity of the output coupler are presented. As expected, the external output power attains much higher values for lower reflectivity but a higher reflectivity enhances the region of lower gain and gives a more uniformly shaped laser emission. Thus, the highest available reflectivity of 99.5% is used in order to achieve a tuning range as wide and steady as possible. A wavelength range from 1020 to 1055 nm is covered.

A problem was thermal strain produced inside the thick birefringent filter by absorption of radiation. The intrinsic absorption of infrared light in quartz is very low (approximately 5×10^{-6} cm^{-1} in anhydrous fused quartz) and usually negligible, but due to the very high circulating power inside the resonator (approximately 400 W for an output coupler reflectivity of 99.5% and an output power of 1 W) there is an observable effect. When the temperature of the birefringent filter increases slightly, the wavelength shifts and the power decreases (370 pm wavelength shift, 2.4 W power decrease (40% of power) observed after 35 minutes operation at maximum pump power). In order to induce this wavelength displacement by a thermal change of refractive index and thickness of the quartz plate, a temperature shift of more than 30 K would be necessary. Further investigations to elucidate this effect showed, that neither a measurable thermal lens was formed (M^2 remains near unity and beam waist location constant) nor did the angle of incidence differ from Brewster's angle (reflected power constant). The effect cannot be caused by a displacement of the two elements of the double-stage

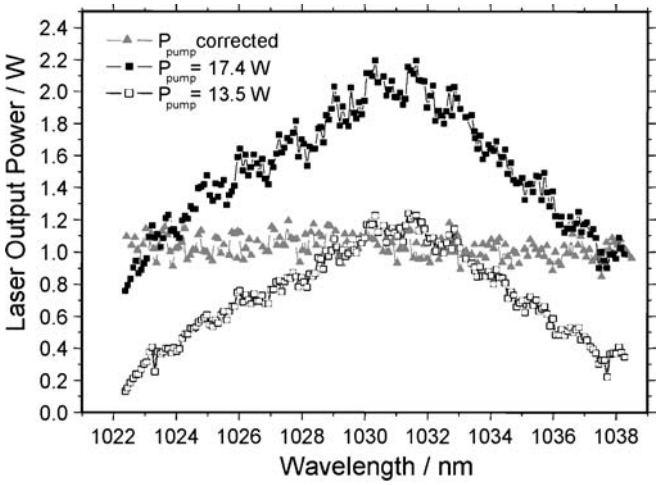

FIGURE 10 Laser output power P_{out} versus wavelength at two different, constant pump power values and for stable output power conditions

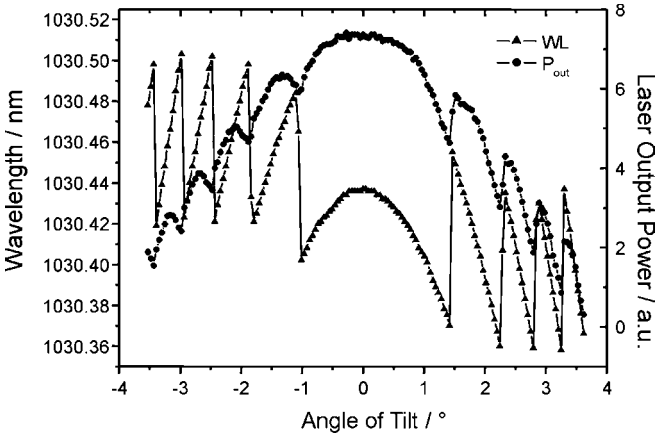

FIGURE 11 Wavelength and laser output power versus etalon angle of tilt with birefringent filter in stationary position

birefringent filter against each other since a single element of equal thickness showed the same behaviour. However, it was observed that the drift could be compensated by realignment. This suggests a small spatial or angular displacement of the beam, caused by the highly asymmetrical heat flow inside the birefringent filter, positioned at Brewster's angle. Thus, we assume that the quartz plate might form a prism and astigmatism might occur.

In order to decrease this thermal strain, it is necessary to limit and adjust the pump power so that the resonator internal power may be maintained at a constant level. Thus, the measured mean output power was limited to a maximum of 1 W, which is sufficient for the application as a seed laser. Figure 10 illustrates the reached output power stabilisation opposed to the output power for two constant pump power values. The automated tuning procedure accomplishes the wavelength selection by adjustment of the appropriate pump power, the rotation of the birefringent filter, according to a beforehand acquired calibration curve and the fine tuning by tilting the etalon. In order to reach each single axial mode within the tuning range, it is essential to align the position of the birefringent filter according to the position of the etalon.

In Fig. 11 the tuning behaviour during the tilting of the etalon is presented. Starting from the position in which the

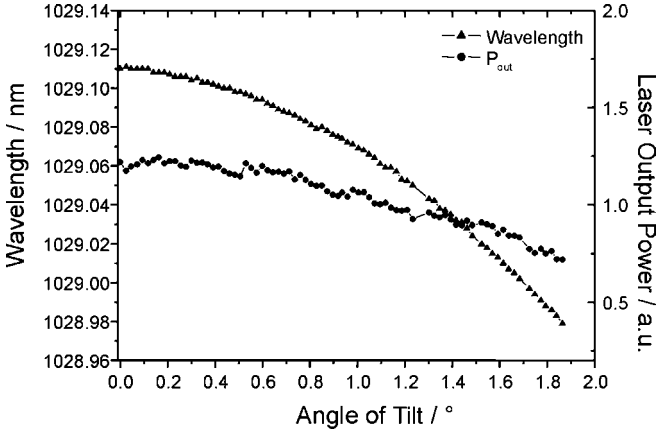

FIGURE 12 Wavelength and laser output power versus etalon angle of tilt. Birefringent filter and output coupler were readjusted during tuning

etalon is oriented parallel to the output coupler, the tuning works only towards shorter wavelengths, since the absolute value of the angle of tilt defines the selected mode. According to theory it is possible to tune the wavelength up to one FSR of the etalon (91 pm for 4 mm thick etalon) if the birefringent filter is retained at a constant position. Then the loss for the current axial mode exceeds the loss for the adjacent mode. This causes the laser emission to hop to the next mode frequency, indicated by a shift in wavelength and higher output power. However, the previously mentioned losses due to resonator misalignment due to beam displacement cause an earlier hopping. In Fig. 12 the improved tuning process is simulated. The positions of the birefringent filter as well as the output coupler were corrected just before the next mode begins to oscillate. This enlarges the tuning range and demonstrates tuning over more than one FSR of the etalon.

4 Conclusion

The Yb:YAG thin disk laser provides a Gaussian spatial mode structure even at high laser power. The existing axial modes next to the central wavelength are separated by a relatively large gap (hundreds of picometers) due to the effect of spatial hole burning combined with the geometry of the thin disk laser resonator. This justifies the performance of the chosen wavelength selection system, which consists of two mechanically bonded birefringent filters for coarse selection and an etalon for fine tuning. This approach requires the adjustment of only two separate units during the tuning procedure, which is an important advantage for automated tuning. Thanks to this combination, the laser emission is narrowed to a spectral range of less than 0.28 GHz (1 pm at 1030 nm). Other axial modes are suppressed effectively. Due to the simultaneous adjustment, the high requirements for the tuning step width are met and the application as seed laser is enabled. It is possible to tune the frequency range of 9.75 THz (1020 to 1055 nm) in 0.47 GHz steps (1.7 pm at 1030 nm). This complies with the selection of one single axial mode. A limitation of output power is introduced to reduce the effects upon the filters due to thermally induced refractive index profiles. This does not represent any drawback for this application since an output power of 1 W is sufficient. Furthermore, the reflectiv-

ity of the output coupler is optimised to improve the tuning characteristics and the range of the wavelength tunability.

ACKNOWLEDGEMENTS The authors kindly appreciate financial support of the "Deutsches Zentrum für Luft- und Raumfahrt" (DLR) under contract 50WP0004.

REFERENCES

1 E.W. Rothe, P. Andresen, Appl. Optics **36**, 3971 (1997)
2 W. Triebel, Space Forum **4**, 121 (1998)
3 A. Giesen, H. Hügel, A. Voss, K. Wittig, U. Brauch, H. Opower, Appl. Phys. B **58**, 365 (1994)
4 U. Brauch, A. Giesen, M. Karszewski, C. Stewen, A. Voss, Opt. Lett. **20**, 713 (1995)
5 A. Giesen, U. Brauch, I. Johannsen, M. Karszewski, U. Schiegg, C. Stewen, A. Voss, OSA Trends in Optics and Photonics Vol. 10 Advanced Solid State Lasers, 280 (1997)
6 M. Karszewski, S. Erhard, T. Rupp, A. Giesen, OSA Trends in Optics and Photonics Vol. 34 Advanced Solid State Lasers, 70 (2000)
7 D. Grebner, D. Müller, W. Triebel, J. König, SPIE **4448**, 16 (2001)
8 W. Paa, W. Triebel, SPIE **5460**, 91 (2004)
9 A. Giesen, U. Brauch, M. Karszewski, C. Stewen, A. Voss, OSA Trends in Optics and Photonics Vol. 1 Advanced Solid State Lasers, 11 (1996)
10 W. Demtröder, *Laser Spectroscopy: Basic Concepts and Instrumentation* 2nd edn. (Springer, Berlin Heidelberg 1996)
11 X.L. Wang, J.Q. Yao, Appl. Opt. **31**, 4505 (1992)
12 H.G. Danielmeyer, IEEE J. Quantum Electron. **6**, 101 (1970)
13 D.R. Preuss, J.L. Gole, Appl. Opt. **19**, 702 (1980)
14 G.J. Kintz, T. Baer, IEEE J. Quantum Electron. **26**, 1457 (1990)